

PARAMETERIZATION AND OPTIMIZATION OF THE ERROR
PROPAGATION IN STAR TRACKERS FOR BUDGET-CONSTRAINED
CUBESATS

A Thesis presented to
the Faculty of California Polytechnic State University,
San Luis Obispo

In Partial Fulfillment
of the Requirements for the Degree
Master of Science in Aerospace Engineering

by
Gagandeep Thapar

June 2023

© 2023
Gagandeep Thapar
ALL RIGHTS RESERVED

COMMITTEE MEMBERSHIP

TITLE: Parameterization and Optimization of the
Error Propagation in Star Trackers for
Budget-Constrained CubeSats

AUTHOR: Gagandeep Thapar

DATE SUBMITTED: June 2023

COMMITTEE CHAIR: Leo Torres, Ph.D.
Professor of Aerospace Engineering

COMMITTEE MEMBER: John Bellardo, Ph.D.
Professor of Computer Science

COMMITTEE MEMBER: Kira Abercromby, Ph.D.
Professor of Aerospace Engineering

COMMITTEE MEMBER: Eric Mehiel, Ph.D.
Professor of Aerospace Engineering

TABLE OF CONTENTS

	Page
LIST OF FIGURES	v
CHAPTER	
1 The Fundamental Question	1
2 The Literature	3
2.1 Background Knowledge and Context	3
2.2 Errors in Star Trackers	10
BIBLIOGRAPHY	23
APPENDICES	

LIST OF FIGURES

Figure		Page
2.1	Sample star catalog entry from Yale Bright Star Catalog	8
2.2	Sample modified star catalog using inter-star angle identification . .	9
2.3	Working principle of the star tracker system [1]	9
2.4	Centroinding errors for various Gaussian-blurred stars	18
2.5	Flow of information through the composite model results in an estimated accuracy, \bar{q}	22

Chapter 1

THE FUNDAMENTAL QUESTION

Observing and measuring nature are the basic tools we can use to characterize the world around us. We can use increasingly accurate sensors to measure different properties of the universe, however, we must come to terms with a fundamental reality. True values of these measurements are non-observable, that is, we can never verify our measurements in nature and are doomed to contain some error in our work. We can attribute these errors to our measurement techniques and the idea that we only have discrete tools trying to measure a continuous reality.

In space, a key property to measure is the attitude, or orientation, of our spacecraft. The direction we point in is imperative for a variety of reasons such as pointing for power generation, pointing to observe interesting phenomena, and pointing to survive the environment. One such sensor to measure our attitude is the star tracker; a clever technology that utilizes the positions of the stars in the universe to ascertain its attitude. The star tracker, similar to any other sensor, is laden with pitfalls in its measurement process and, due to a variety of factors, is prone to error. Before we move forward, we must determine why analyzing the error propagation in a star tracker is worth doing; what will benefit from studying how star trackers err.

CubeSats

CubeSats, developed by the Cal Poly CubeSat Lab in 1999 by Prof. Jordi Puig-Suari and Prof. Bob Twiggs, have long been used as a bus for university programs and commercial businesses to fly experiments in Low Earth Orbit, or, LEO. CubeSats

typically use COTS, or commercial-off-the-shelf, components as they're characterized by their ease and low-cost of development. While CubeSats have typically been used for simpler observation missions, the technology has been maturing and, as a consequence, as have their mission requirements. Attitude determination and control have been an increasingly popular requirement imposed on CubeSats as a means to accomplish more complex missions i.e., optical-communication demonstrations (SOTA, OSIRISv2)[2]. With the attitude determination requirements becoming increasingly stringent, the sensor selection space converges to only a few select types considering the constraints CubeSat developers are forced to deal with such as lack of payload volume, limited power options, and especially total cost. Star trackers are a prime example of a sensor that fits the mission criteria but are overlooked due to their cost. Star trackers for CubeSats can start at \$30,000 and only go up from there; a cost that can sometimes equal if not be greater than the total budget for a mission. However, with attitude determination requirements becoming stricter, a need for a low-cost solution emerges.

The fundamental question to ask is whether or not a star tracker, traded on performance for cost, is a viable solution for CubeSat attitude determination in the future. This thesis aims to answer the question by analyzing where errors exist, how they propagate, and how different hardware can influence the expected attitude accuracy.

Chapter 2

THE LITERATURE

2.1 Background Knowledge and Context

CubeSats and Pointing

Since their inception in 1999, CubeSats have been employed for a variety of mission types. From measuring elements in the Earth's exosphere, to testing vibration and dampening experiments in microgravity, to experimenting accelerated deorbit times via dragsail [3], it's clear to see that CubeSats are not pigeonholed into a single mission archetype. However, as the technology has matured and missions become more complex, their requirements, especially for pointing, have become stricter.

CubeSats, being developed at a university, continue to be designed at universities such as California Polytechnic State University - San Luis Obispo (Cal Poly SLO) or University of California - Davis (UC Davis). The initial design made it possible for organizations with limited resources and funding to still be able to develop functional spacecraft with unique mission objectives. While CubeSats have emerged into the greater market and can be developed with upwards of \$1 Million, typical budget-constrained or university CubeSat programs can be expected to spend on the order of \$50,000 - \$200,000 [4]. While a large sum of funds, it should be noticed that a CubeSat is a complicated amalgamation of instruments, supporting avionics, structure, and software, all of which is still expected to undergo and survive testing such as vibration and thermal vacuum tests to comply with launch vehicle standards. Each of these subsystems and requirements requires some amount of the total fund-

ing. As a consequence, funds allocated towards supporting sensors, such as attitude determination sensors, are typically a small portion of the total funding. Despite the limited funding available for such CubeSat programs, technology demands and mission requirements have increased in complexity, creating a need for more affordable component alternatives. Pointing requirements, in specific, have become increasingly strict. As CubeSats continue to demonstrate their capabilities for missions, earth-sensing missions and inter-satellite communication systems have slowly been outsourced from traditional, larger spacecraft to the modern CubeSat. As a result, pointing has become increasingly important to consider and control.

QuakeSat and CLICK

QuakeSat was a mission which would measure and record earthquakes on the surface [5]. The team from Space Systems Development Laboratory (SSDL) reported, for mission success, they used a wide-angle light sensor and magnetometer; they "were not ideal for attitude determination"[5]. Stories like QuakeSat characterize the the early missions of CubeSats - where attitude was not a major concern and, as a consequence, became afterthoughts in the design cycle. With more modern missions, however, attitude has become the forcing function for mission success. The CubeSat Laser Infrared CrosslinK (CLICK) was a technology demonstration for an inter-satellite laser-based communication system from MIT[6]. The demonstration, through analysis of the inter-satellite distance and relative motion, required the pair of CubeSats to point in a single axis to within ± 5.18 arcsec of each other. Another optical mission, ASTERIA, looks to optimize beam pointing control and requires 3.3 arcsec [7] of pointing accuracy to complete its objective. The trend of CubeSats taking on complex technology demonstration and requiring strict pointing requirements has only and will only increase as the confidence in CubeSat technology improves. A

worrying observation, however, is that the list of sensors able to meet requirements is starting to narrow down. Without a suitable sensor, CubeSat capabilities can stagnate indefinitely.

With other sensors, sun sensors, for example, accuracy begins to fall. Sun sensors can be as accurate as 0.1 deg [8], or 360 arcsec, and cost as much as \$9,000 [9]. While sun sensors were once the standard for attitude determination on budget-constrained CubeSats, it's clear that they can no longer fulfill the requirements being imposed on modern day CubeSat mission. On the opposite end of the spectrum, however, star trackers can be as accurate as 5 arcsec but as expensive as \$120,000 [10] or more. CubeSats - particularly developed in university settings or those that are budget constrained - are typically underfunded to afford such star trackers. Other attitude determination alternatives include magnetometers (whose accuracy can vary depending on the orbit type and can be as accurate as 0.01 degrees [11]), horizon sensors (which can be accurate to approximately 0.1 degrees [12]), or passive systems such as gravity-gradient which are only accurate to approximately 15 degrees [13] depending on the construction and mass properties of the spacecraft. While alternatives may be cheaper, it's clear to see that the performance gap compared to star trackers is great and needs to be closed. This gap can be filled by trading on star tracker performance for cost, allowing for more affordable alternative options while still outperforming less expensive sensors. Parameterizing the error in star trackers based on selected hardware and expected environmental conditions are one such method to determine how to perform the performance trade.

Figure plotting star tracker and other attitude sensor cost vs performance

Parameterization of Error

While other approaches in determining how to develop more affordable star trackers are viable, analyzing the error propagation allows us to determine additional information about the system and develop a tool for CubeSat developers. By looking at each physical step of the star tracker from end-to-end, a complete mathematical model of the star tracker can be deduced, including, but not limited to, where errors occur for one reason or another. For example, by identifying flaws in the camera construction such as the normality of the boresight vector or the tilt of the focal array, immediate errors can be characterized and modeled as the ideal model for centroiding would be based on a skewed representation of the celestial sphere. By incorporating different effects, specifically the camera hardware and noise, the algorithmic errors, and the leading environmental errors in low earth orbit (LEO), a model can be devised where a given set of inputs (i.e., from a list of mission requirements) can be used to devise how accurate a theoretical star tracker would be. This black box would enable CubeSat developers to determine if investing in a low-cost star tracker will be sufficient for the mission without needing to experimentally test for it using their expected mission parameters.

Investigating the error propagation also enables us to determine where the most errors are prone to occur and where it is worth the time and resources to optimize a process. By fully understanding and parameterizing the star tracker process, a greater understanding of how to model the star tracker accuracy in on-orbit conditions can be determined and used to drive decision making for attitude determination sensor selection without *a priori* experimental information.

Alternative methods in reducing the cost of the star tracker include optimizing hardware or writing custom firmware for the optical module. While worthwhile efforts,

the same pitfalls of high development costs still persist. Optimizing the hardware will still require some knowledge of how the optical system works and how different decisions and hardware permutations will affect the estimated accuracy. This black box devised through analyzing error propagation allows developers to take the guess work out of the hardware selection and reduces the development cost and time in broad iteration. Software optimization is another alternative, however, without a great understanding of the physics, image analysis process, and flight software knowledge, developing personalized algorithms will prove to be burdensome and can still lead to expensive development cycles. Analyzing the error propagation through a theoretical lens allows us to specifically determine where errors, or losses, are generated and how hardware selection can help mitigate errors. It also enables us to selectively allow errors to persist by choosing affordable hardware, thereby reducing the total cost of the star tracker. It should be clear by now that, due to the rapid maturation of CubeSat technology and capability, a demand for equally capable attitude determination sensors needs to be met, especially one that fits within the confines of a typical CubeSat budget.

The literature offers several suggestions in analyzing the error propagation within the sensor such as hardware considerations, "thermal drift, optical aberration, detector noise"[14], and systematic algorithmic errors. However, before we can analyze where error is prone to occur, we must first understand what a star tracker is and how they work.

What Is a Star Tracker and How Do They Work?

A star tracker is an optical-based sensor that uses the position of stars to determine its attitude; it relies on the notion that relative star movement is low and can

be effectively mapped to each other. This mapping exists within catalogs formulated over several years from different organizations such as the Yale Bright Star Catalog 5 (BSC5). The catalog contains key information such as Star ID, right ascension and declination in the celestial sphere, brightness magnitude, right ascension and declination motion, and other features.

Catalog Number	B1950 Right Ascension	B1950 Declination	Spectral Type	V Magn. x100	R.A. Proper Motion	Dec.Proper Motion	Radial Velocity	Object Name
...								
123	0.138637	0.951592	B8	4.73	2.181662e-07	-4.848137e-08	-	-
124	0.138259	0.922222	K2	5.60	-2.569512e-07	-9.211460e-08	-	-
125	0.137081	-0.851784	A0	4.77	6.932835e-07	8.241832e-08	-	-
...								

Figure 2.1: Sample star catalog entry from Yale Bright Star Catalog

A copy of the catalog can then be modified to include information, called features, such as inter-star angles, ratio of triangle legs created by 3 stars, or even pyramidal information; the specific feature generated is determined by the specific identification method employed. The modified catalog contains the permutations of the stars that comprise the given feature set. The identification algorithm can then be used to identify each star in a given image; once each star is identified, a final calculation to determine the star location and the center of the image is processed and mapped to the original catalog. Given the position of the star in the image, the star tracker can determine its own position (in right ascension and declination) based on the image center (as this is where the boresight of the star tracker lies). The QUEST algorithm can then be used to determine a quaternion representation of the star tracker's attitude from the right ascension and declination.

Onboard the star tracker, images are captured of the stars and processed by the star tracker. During the centroiding process, the star tracker will read the image and determine where the stars are located within the image plane. It will then create the

Star A ID	Star B ID	$\cos(\text{Inter-star Angle})$
...		
123	124	-
123	125	-
124	125	-
...		

Figure 2.2: Sample modified star catalog using inter-star angle identification

aforementioned features and store it in memory. During the identification process, the features in memory are recalled and compared to against the modified catalog where potential matches are found. Once a suitable match, typically characterized by high likelihood of similarity in combination with a filter, the attitude is recalled from the entry in the modified catalog. It is not uncommon for the star tracker to fail in finding a sufficiently confident match due to the nigh-infinite number of variations a single feature set can have due to image positioning and centroiding errors. To combat this, star trackers typically take multiple images per second to try to find better matches. This process repeats indefinitely and will generate high-accuracy determinations of attitude.

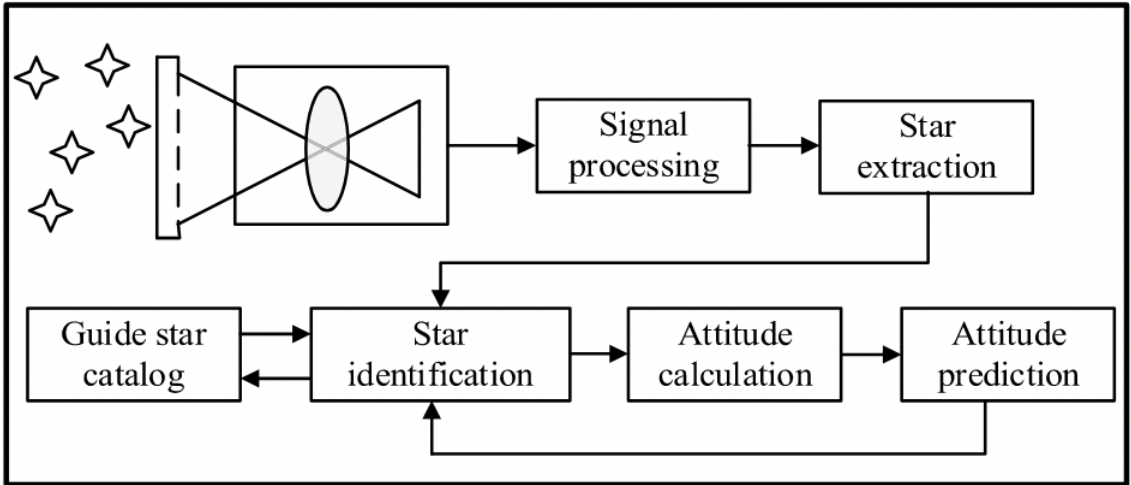


Figure 2.3: Working principle of the star tracker system [1]

The star tracker, in addition to its 2 main process phases, has 2 operating phases. If the star tracker has some *a priori* knowledge of its attitude in recent time, i.e., based on previous star tracker readings, then the star tracker only has to search a small portion of the modified catalog in order to find a match as the catalog can be ordered by attitude. If, however, the star tracker has no *a priori* knowledge of its attitude, i.e., post-detumble, then the star tracker must search the entire modified catalog. Because the modified catalog is so large and can contain a great number of combinations for an even greater number of stars, the process to determine the attitude can take significantly longer. This operating phase is typically called the *Lost in Space* problem and is a unique metric in comparing star tracker performance.

2.2 Errors in Star Trackers

Now that we understand what a star tracker is and how they work, it's imperative to describe what error propagation is and how it affects the star tracker. Error propagation is “a basic problem analyzing the uncertainty of reliable systems”[15]; we want to determine why a star tracker is not totally accurate, where errors originate, and how they persist through the star tracker process to affect its final estimated accuracy. According to Jia et al. (2010), “[t]he most important factors that affect star tracker accuracy include thermal drift, optical aberration, detector noise, and systematic error of star image centroid estimation algorithm”[14]. We can characterize these errors by analyzing the physics behind their presence and how different factors affect their intensity. Following the advice of Jia et al. (2010), this thesis aims to analyze errors due to the optical system hardware defects, optical sensor noise, algorithmic assumptions and errors, and the thermal environment of LEO, and how each error tracks through the attitude determination process and its affect on the expected accuracy.

Hardware Limitations

The physical hardware of the star tracker will always be the first source of error and will be compounded upon throughout the process. Inaccuracies in the optical axis, focal plane flatness, and lens distortion all contribute to errors in the centroiding process, leading to errors in attitude determination. Camera calibration is a common technique to reduce hardware inconsistencies propagating error through the attitude determination model. Sun et al. (2013), proposes a model to handle the uncertainty of where the incident light rays from the navigation stars fall on the focal plane. [16]

$$\xi_A = \left(\frac{\left(\frac{f + \Delta f + \Delta s \tan(\theta)}{\cos(\theta + \beta_{ri})} * \sin(\beta_{ri}) + \frac{\Delta s}{\cos(\theta)} + \Delta x + \Delta d \right)}{f} \right) - \arctan\left(\frac{\Delta s}{f \cos(\theta)}\right) - \beta_{ri} \quad (2.1)$$

where

ξ_A defines the star tracker measurement accuracy

f represents the focal length of the star tracker

Δs represents the deviation of the optical axis with respect to the boresight

Δx represents the star point-extraction error

Δd represents radial distortion in the lens

β_{ri} represents the angle between the optical axis and incident light ray

θ represents in the inclination of the focal plane

Error due to the optical system hardware can be presented via Monte Carlo Analysis. Sun et al. (2013) imposes a zero-mean error for all properties with varying levels of standard deviation as shown in Table 2.1

Parameter	Mean Distribution	Deviation (Gaussian)
Error of Star Point Extraction	0	0.1/3 pixels
Error of Principal Point	0	4.5/3 pixels
Error of Focal Length	0	0.6/3 pixels
Error of Inclination Angle	0	0.075°/3
Distortion	0	0.1/3 pixels

Table 2.1: Distribution of parameters as presented in Sun et al. (2013)[16]

While Sun et al. (2013) devised this model to generate estimated attitude determination accuracy, it should be noted that only hardware limitations were considered. In addition to the inaccuracies of the focal system on the star tracker, additional considerations from Liu et al. (2010) address radial distortion, decentering, and thin prism distortions [17]

$$\begin{bmatrix} \delta_u(u', v') \\ \delta_v(u', v') \end{bmatrix} = \begin{bmatrix} u' \\ v' \end{bmatrix} - \begin{bmatrix} u \\ v \end{bmatrix} = \begin{bmatrix} (g_1 + g_3)u'^2 + g_4u'v' + g_1v'^2 + \kappa u'(u'^2 + v'^2) \\ g_2u'^2 + g_3u'v' + (g_2 + g_4)v'^2 + \kappa v'(u'^2 + v'^2) \end{bmatrix} \quad (2.2)$$

where

$[g_1, g_2, g_3, g_4]$ each represent a different distortion property.

Modeling the physical error of the image-capturing process of the star tracker will cause compounding errors down the propagation analysis and should be closely studied. Creating an valid accuracy range based solely on the physical process will lighten difficulty and computation for analyzing further errors, i.e., the ones caused by algorithms. A multivariate propagation analysis approach will likely be best to use for modeling the physical properties as many of the affects are co-dependent on each other and can change constantly. A major source of fluctuation, for example, is

the expansion or compression of the focal length due to the thermal environment in LEO.

Thermal Effects

One of the larger effects from the environment is the rapidly changing thermal environment. In Low-Earth Orbit, or, LEO, spacecraft can experience a temperature swing between -65C and +125C[18] which can cause thermal stresses on all hardware. For star trackers in particular, the lens is of interest when analyzing thermal cycles. For one, the lens can change shape, lengthening or shortening the focal length in times of extreme heat or cold respectively. Jamieson et al. (1981) thoroughly describes the relation between optical systems and thermal effects, especially noting how the focal length changes with temperature [19]

$$x_f = \frac{1}{f} \frac{df}{dt} = x_g - \frac{1}{n - n_{air}} \left(\frac{dn}{dt} - n \frac{dn_{air}}{dt} \right) \quad (2.3)$$

$$n_t - 1 = (n_{15} - 1) \left(\frac{1.0549}{1 + 0.00366t} \right) \quad (2.4)$$

$$(n_{15} - 1) * 10^8 = 8342.1 + \frac{2406030}{130 - \nu^2} + \frac{15996}{38.9 - \nu^2} \quad (2.5)$$

$$n_{abs} = n_{rel} n_{air} \quad (2.6)$$

$$x_g = \frac{1}{R_1} \frac{dR_1}{dt} = \frac{1}{R_2} \frac{dR_2}{dt} \quad (2.7)$$

where

f is the focal length

x_g is the change of surface radii of the lens with respect to temperature

n is the refractive index at a given temperature

n_{air} is the refractive index of air $\equiv 1.0$

Thermal expansion will directly affect the hardware and, in turn, will influence centroiding processes. Immediately, it's clear to see that focal length is a function of the thermal environment; seeing that the focal length is one of the most important and relevant parameters of the star tracker, it's possible to use this temperature-dependent function in place of where focal length is being called. This composite allows us to introduce a new dependent variable in equations that were previously stagnant, i.e., in the hardware limitations posed by Sun et al. (2013) in Equation 2.1. Temperature can be seen as a function of the absorptivity and emissivity of the system in orbit where the eclipse times will determine the max temperature the system can reach. Depending on the range of temperatures the system will experience, especially so often due to the short orbital period in LEO, the lens of the system may see drastic degradation and changes over time, widening the accuracy range.

CCD Noise

Sensor noise, specifically from the CCD, is another factor we must analyze when determining how our system and the environment affect attitude determination. CCD Noise often appears as partially illuminated pixels in the absence of a real incident light and is caused by the noise in the Analog to Digital Converter during the image capture process. G.E. Healey et al. (1994) proposes a model that relates the irradiance, dark current, and quantization to the expected noise level in a given pixel[20].

$$D(a, b) = \mu(a, b) + N(a, b) \quad (2.8)$$

$$N(a, b) = N_I(a, b) + N_C(a, b) \quad (2.9)$$

where

D represents the digital value of a pixel at location (a, b) on the focal plane

$\mu(a, b)$ represents the expected digital value based on standard camera principles

$N(a, b)$ represents the noise of a given pixel

$N_I(a, b)$ represents the noise part that varies with the image

$N_C(a, b)$ represents the noise part that is invariant of the electrons captured

CCD Noise is composed of several different sources, as alluded to within Equation 2.9 such as unintentional light scattering from other bodies, analog-digital converter noise, and Dark Current. Dark Current is a form of CCD Noise that is a result of residual electric current in the pixel buckets while there is no incident light being projected on the focal plane. Dark Current can worsen with age of the sensor, among other factors.

Healey et al. (1994) proposes a model to account to account for different noises in CCD sensors.

$$D_C(a, b) = \left(I(a, b) + \frac{N_S(a, b)}{\hat{K}(a, b)} + \frac{N_R(a, b)}{\hat{K}(a, b)} \right) A + \frac{N_Q(a, b)}{\hat{K}(a, b)} \quad (2.10)$$

where

D_C represents the corrected digital value of a pixel at location (a, b)

I represents the irradiance on a given pixel

N_S represents shot noise, a type of noise that deals with the uncertainty of the number of electrons captured

N_R represents zero-mean amplifier noise

N_Q represents noise from the quantization process

\hat{K} represents the estimate of number of captured photoelectrons

CCD Noise varies between cameras and can come in the form of several kinds of noises. To reduce noise (and improve centroiding), it's important that the noise be calculated to set a *Noise Floor*, or a filter that attempts to remove as much noise from the image without removing stars. A typical Noise Floor can be calculated using the average and standard deviation of the brightness of the pixels in the image [21]:

$$NF = \bar{B} + 5 * \sigma_B \quad (2.11)$$

where

\bar{B} represents the average brightness value

σ_B represents the standard deviation in brightness

The Noise Floor is a parameter that is typically calculated during operation and will change between image captures. This ensures the Noise Floor is not over-filtering clean photos or under-filtering noisy photos. The noise will be important to consider as it directly affects what the centroiding step considers a star or not which can drive error extremely high.

Algorithmic Errors

One of the largest errors occurs during the algorithmic processes. Centroiding is a sensitive process that is limited by the pixel density of the focal array. Yang et al. (2011) proposes a novel approach of analyzing the frequency domain of the centroiding function to reduce the pixel accuracy from 0.06 to 6×10^{-5} pixels [22]. Because the centroiding process relies on analyzing the brightness of each pixel, its quite common for the process to select a random point around inside the star as opposed to the true center. Even small errors in this process will propagate through the identification and quaternion generation steps. Most centroiding algorithms approach the problem using the *Center-of-Mass* approach where the "center of mass" of the star (using the brightness value of the pixel) is used; i.e.,

$$\begin{aligned}\hat{x}_c &= \frac{\iint_W x I(x, y) dx dy}{\iint_W I(x, y) dx dy} \approx \hat{x}_g = \frac{\sum_{i=1}^n x_i I_i}{\sum_{i=1}^n I_i} \\ \hat{y}_c &= \frac{\iint_W y I(x, y) dx dy}{\iint_W I(x, y) dx dy} \approx \hat{y}_g = \frac{\sum_{i=1}^n y_i I_i}{\sum_{i=1}^n I_i}\end{aligned}\tag{2.12}$$

where (\hat{x}_c, \hat{y}_c) is the ideal centroid of the star if the measurement system was continuous and (\hat{x}_g, \hat{y}_g) is the expected centroid due to the discretization of the pixels. Analyzing how the stars are purposefully blurred in the image also dramatically changes how accurate the centroiding algorithm can be. In order to accurately determine the centroid of a star, the optical system is purposefully blurred or defocused which enables the stars to occupy more space than it would otherwise. The radius of the blur is typically a Gaussian, or uniform, function whose width can be modulated by the software. With greater Gaussian widths, more pixels are occupied by the star which can lead to additional error as seen in Figure 2.4 [22].

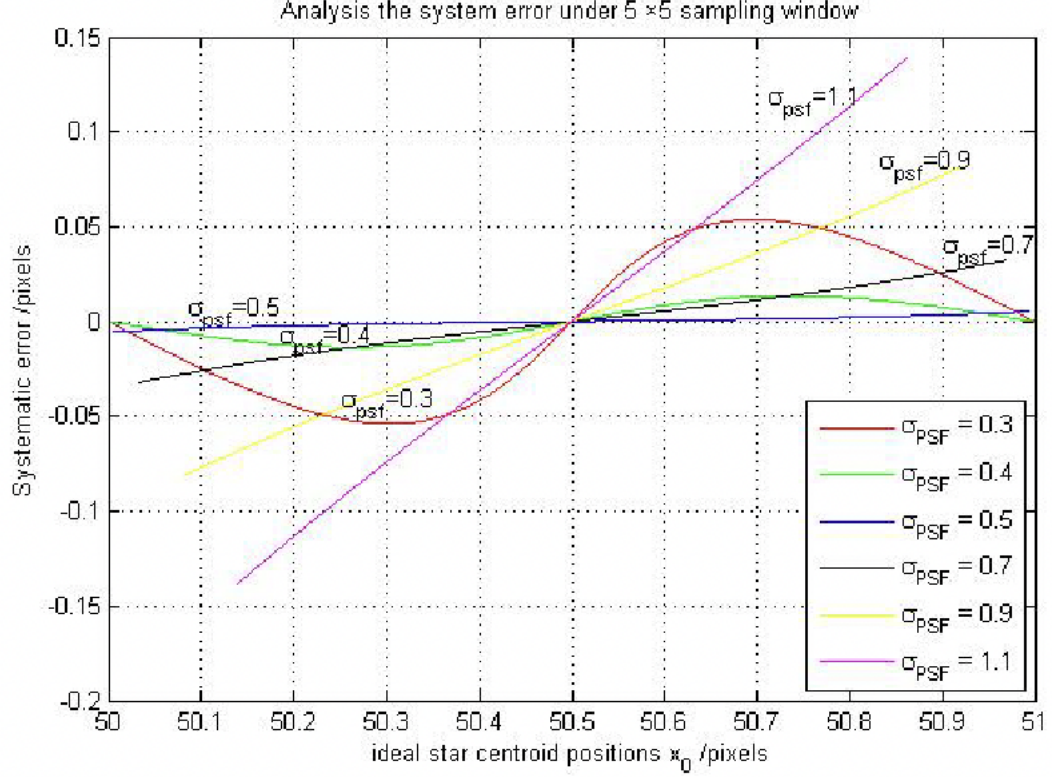


Figure 2.4: Centroiding errors for various Gaussian-blurred stars

Additional considerations are taken into account such as the likelihood of multiple stars being close together and creating larger centroiding-based errors or noise causing the centroiding algorithm to identify a false star. These are mainly dealt with on an implementation-by-implementation basis but it can easily be seen how star identification can be askew as a consequence of failing to consider the edge cases. Analyzing a discrete set of Gaussian widths in the Monte Carlo Analysis tool can help pair various widths with the hardware as it's unclear if there's necessarily a "best" Gaussian width to choose for all systems.

Error Propagation Techniques

While modeling the errors in the star tracker is a significant part in the analysis, determining how the error propagates through the system and its affect on its accuracy

is a different and equally important step to understand; how do the aforementioned errors compound together throughout the process. A common method in modeling errors is to say that for a measurement, x , we can say

$$x = \mu_x + e_x \quad (2.13)$$

where μ_x represents the mean or expected value of the measurement and e_x is a zero-mean random variable with some standard deviation, σ_x [23]. In the context of star trackers, this could represent a multitude of measurements such as the brightness of a given pixel given the direct light from the star and the random addition or subtraction of pixel amplitude due to CCD noise or Dark Current. Modeling measurements as the sum of some true value and random variance allows for various models to be combined and have some accuracy range attached to it. For example, if a pixel's brightness is said to be 1000 ± 10 nits and a coarse physical filter lowers the brightness by 20.00 ± 5.00 %, we can say that the new pixel brightness is $\bar{B} = 900 \pm 12.247$ nits as given by

$$\bar{Q} = ab + \sqrt{\sigma_a^2 + \sigma_b^2} \quad (2.14)$$

where Q is the estimated measurement value and σ_a and σ_b are the standard deviations of the measurements.

The model for combining measurement uncertainties in (2.14) is useful in showing how simple models which are independent of one another compound together. In the case where different models are more complicated and are co-dependent on each other, a different approach is required. As posed in Burns et al. (1997), a Multivariate Linear Transformation technique allows a list of output measurements, \mathbf{y} , to be rep-

resented as a vector of size n -by-1 which is said to be the product of the independent measurements, \mathbf{x} , another n -by-1 vector, and the co-variance matrix; i.e.,

$$\mathbf{y} = \mathbf{A}\mathbf{x} \quad (2.15)$$

where the covariance matrix of \mathbf{y} , Σ_y , is proportional to the covariance matrix of \mathbf{x} , Σ_x ; i.e.,

$$\Sigma_y = A\Sigma_x A^T \quad (2.16)$$

where

$$\Sigma_x = \begin{bmatrix} \sigma_{11} & \sigma_{12} & \dots & \sigma_{1n} \\ \sigma_{21} & \sigma_{22} & \dots & \sigma_{2n} \\ \vdots & & \ddots & \vdots \\ \sigma_{n1} & \sigma_{n2} & \dots & \sigma_{nm} \end{bmatrix} \quad (2.17)$$

where A is a matrix of weights relating the input to output measurements and σ_{ij} , is the covariance between measurement i and j [23]. This technique will enable models which contain co-dependent information to be compounded together; i.e., in the case of modeling the relation between thermal expansion/compression of the lens and its affect on centroiding accuracy.

Error Analysis Alternatives: Monte Carlo Analysis

Error propagation via Multivariate Linear Transformation, while powerful and can maintain complex relations between various parameters, requires great understanding of the underlying physics and interdependencies. A feasible alternative to reducing required knowledge for error propagation is by employing Monte Carlo Analysis. Monte Carlo Analysis is a technique where experimental probabilistic trials are run to determine estimations of a measurement given sets of input parameters and their expected values and variance [24]. This technique allows us to run trials with varying inputs and generate an estimated accuracy without requiring advanced knowledge of the co-dependence of some of the parameters.

Contributions to the Field

As we can see, it is non-trivial to determine how imperfections in the star tracker affect its accuracy. Analyzing error propagation allows us to step through how accuracy changes with each process and determine which errors are forced to exist due to the discretization of the celestial sphere. Developing a tool for CubeSat developers to estimate accuracy allows them to determine if and how various hardware options meet their mission requirements, allowing them to sink less costs for sensor development. While the main goal of this thesis is to develop a tool to analyze star tracker accuracy given a few parameters, another objective is to inform developers of major considerations. By looking at how errors stack up, decisions can be made to determine if it's worth the effort, cost, or time to optimize some process. We hope that the content allows star tracker development cycles to accelerate, further reducing cost of the final product.

Conclusion

While the literature offers several options to model accuracy of various subprocesses in the star tracker, the main challenge will be combining the information to produce a single system to ingest mission parameters and output estimated accuracy. As such, additional review of statistics in stochastic processes and multivariate error analysis will be required to accurately combine information together. Monte Carlo Analysis will supplement the multivariate transformation by looking at several unique permutations of inputs to determine an estimated accuracy uncertainty.

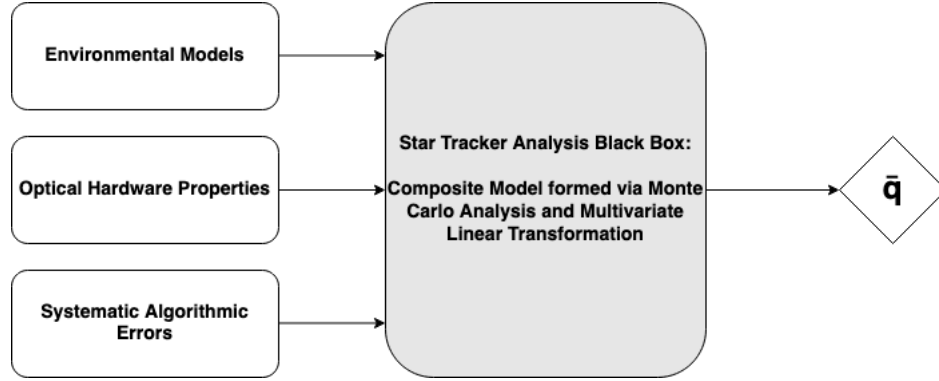


Figure 2.5: Flow of information through the composite model results in an estimated accuracy, \bar{q}

Validation of composite models will be proven mathematically as experimental trials require additional care in maintaining control groups and calibration. Validation can also take the form of comparison between the devised models and advertised star tracker performance given their physical characteristics. Parameterizing these errors as functions of similar variables allows for the development of a tool to generate the estimated accuracy, or uncertainty, of a star tracker given a few mission parameters. Herein lies the goal of the thesis; to synthesize the previously studied models and combine them to analyze errors in star trackers and track their presence and intensity through the process.

BIBLIOGRAPHY

- [1] Yongyong Li, Xinguo Wei, Jian Li, and Gangyi Wang. Error correction of rolling shutter effect for star sensor based on angular distance invariance using single frame star image. *IEEE Transactions on Instrumentation and Measurement*, 71:1–13, 2022.
- [2] Alberto Carrasco-Casado, Abhijit Biswas, Renny Fields, Brian Grefenstette, Fiona Harrison, Suzana Sburlan, and Morio Toyoshima. Optical communication on cubesats — enabling the next era in space science. In *2017 IEEE International Conference on Space Optical Systems and Applications (ICSOS)*, pages 46–52, 2017.
- [3] PolySat. Missions launched, 2015.
- [4] Anders Nervold, Joshua Berk, Jeremy Straub, and David Whalen. A pathway to small satellite market growth. *Advances in Aerospace Science and Technology*, 01:14–20, 01 2016.
- [5] Matthew Long, Allen Lorenz, Greg Rodgers, Eric Tapio, Glenn Tran, Keoki Jackson, Robert Twiggs, T.E. Bleier, and Stellar Solutions. Ssc02-ix-6 a cubesat derived design for a unique academic research mission in earthquake signature detection. 10 2022.
- [6] Peter Grenfell, Alexa Aguilar, Kerri Cahoy, and Michael Long. Pointing, acquisition, and tracking for small satellite laser communications. 2018.
- [7] Ondrej Čierny and Kerri L Cahoy. On-orbit beam pointing calibration for nanosatellite laser communications. *Optical Engineering*, 58(4):041605, 2018.

- [8] Josh O'Neill, Nadja Bressan, Grant Mcorley, and Nicholas Krouglicof.
Development of a high-accuracy low-cost sun sensor for cubesat application.
Aeronautics and Aerospace Open Access Journal, 4:142–146, 09 2020.
- [9] CubeSatShop. Bison64-et.
- [10] Rocket Lab. St-16rt2 star tracker.
- [11] Nils Olsen. Magnetometer data from the grace satellite duo. *Earth, Planets and Space*, 73(1):62, Mar 2021.
- [12] Mohamad Dol Bahar, Mohd Effandi, Mohd Khair Bin Hassan, Norhizam Hamzah, Ahmad Sabirin Arshad, Xandri C. Farr, Lourens Visagie, and Willem H. Steyn. Modular cmos horizon sensor for small satellite attitude determination and control subsystem. 2006.
- [13] Dmitry Roldugin and Michael Ovchinnikov. Dual-spin satellite motion in magnetic and gravitational fields. *Keldysh Institute Preprints*, page 20, 01 2015.
- [14] Hui Jia, Jiankun Yang, Xiujian Li, Juncai Yang, MengFei Yang, YiWu Liu, and YunCai Hao. Systematic error analysis and compensation for high accuracy star centroid estimation of star tracker. *Science China Technological Sciences*, 53:3145–3152, 11 2010.
- [15] Jianfang Zhang. The calculating formulae, and experimental methods in error propagation analysis. *IEEE Transactions on Reliability*, 55(2):169–181, 2006.
- [16] Ting Sun, Fei Xing, and Zheng You. Optical system error analysis and calibration method of high-accuracy star trackers. *Sensors (Basel, Switzerland)*, 13:4598–623, 04 2013.

- [17] HaiBo Liu, Xiujian Li, Ji-Chun Tan, Jian-Kun Yang, Jun Yang, De-Zhi Su, and Hui Jia. Novel approach for laboratory calibration of star tracker. *Optical Engineering*, 49:3601–, 07 2010.
- [18] Dynamic Range Corporation Jeannette Plante, Brandon Lee. Environmental conditions for space flight hardware - a survey, 2004.
- [19] Thomas H Jamieson. Thermal effects in optical systems. *Optical Engineering*, 20(2):156–160, 1981.
- [20] G.E. Healey and R. Kondepudy. Radiometric ccd camera calibration and noise estimation. *IEEE Transactions on Pattern Analysis and Machine Intelligence*, 16(3):267–276, 1994.
- [21] C.C. Liebe. Accuracy performance of star trackers - a tutorial. *IEEE Transactions on Aerospace and Electronic Systems*, 38(2):587–599, 2002.
- [22] Jun Yang, Bin Liang, Tao Zhang, and Jingyan Song. A novel systematic error compensation algorithm based on least squares support vector regression for star sensor image centroid estimation. *Sensors (Basel, Switzerland)*, 11:7341–63, 12 2011.
- [23] Peter D. Burns and Roy S. Berns. Error propagation analysis in color measurement and imaging. *Color Research & Application*, 22(4):280–289, 1997.
- [24] Christos E. Papadopoulos and Hoi Yeung. Uncertainty estimation and monte carlo simulation method. *Flow Measurement and Instrumentation*, 12(4):291–298, 2001.

- [25] Juan Shen, Guangjun Zhang, and Xinguo Wei. Simulation analysis of dynamic working performance for star trackers. *Journal of the Optical Society of America. A, Optics, image science, and vision*, 27:2638–47, 12 2010.